Title	The fluted giant clam (Tridacna squamosa) increases the protein abundance of the host's copper-zinc superoxide dismutase in the colorful outer mantle, but not the whitish inner mantle, during light exposure
Author(s)	Shit F. Chew, Clarissa Z. Y. Koh, Kum C. Hiong, Mel V. Boo, Wai P. Wong and Yuen K. Ip
Source	*Comparative Biochemistry and Physiology Part A: Molecular & Integrative Physiology*, *250*, Article 110791
Published by	Elsevier

The fluted giant clam (*Tridacna squamosa*) increases the protein abundance of a host's copper-zinc superoxide dismutase in the colorful outer mantle, but not the whitish inner mantle, during light exposure

Shit F. Chew[1,*], Clarissa Z. Y. Koh[2], Kum C. Hiong[2], Mel V. Boo[2], Wai P. Wong[2] and Yuen K. Ip[2]

[1]Natural Sciences and Science Education, National Institute of Education, Nanyang Technological University, 1 Nanyang Walk, Singapore 637616, Republic of Singapore

[2]Department of Biological Sciences, National University of Singapore, Kent Ridge, Singapore 117543, Republic of Singapore

*author for correspondence (E-mail: sfun.chew@nie.edu.sg)

Running head: CuZnSOD in *T. squamosa*

Correspondence address:

Dr. S. F. Chew
Associate Professor
Natural Sciences and Science Education
National Institute of Education
Nanyang Technological University
1 Nanyang Walk
Singapore 637616
Republic of Singapore

Phone: (65)-67903829
Fax: (65)-68969414
Email: sfun.chew@nie.edu.sg

Abstract

The colorful outer mantle of giant clams contains abundance of symbiotic dinoflagellates (zooxanthellae) and iridocytes, and has direct exposure to light. In light, photosynthesizing dinoflagellates produce O_2, and the host cells in the outer mantle would be confronted with hyperoxia-related oxidative stress. In comparison, the whitish inner mantle contains few symbiotic dinoflagellates and no iridocytes. It is involved in shell formation, and is shaded from light. CuZnSOD is a cytosolic enzyme that scavenges intracellular $O_2^{\bullet-}$. We had obtained from the outer mantle of the fluted giant clam, *Tridacna squamosa*, the complete cDNA coding sequence of a host-derived *copper zinc superoxide dismutase* (*CuZnSOD*), which comprised 462 bp and encoded for 154 amino acids with a MW of 15.6 kDa. *CuZnSOD* was expressed strongly in the outer mantle, ctenidium, hepatopancreas and kidney. The transcript level of *CuZnSOD* remained unchanged in the outer mantle during light exposure, but the protein abundance of CuZnSOD increased ~3-fold after exposure to light for 6 or 12 h. By contrast, 12 h of light exposure had no significant effects on the gene and protein expression levels of *CuZnSOD*/CuZnSOD in the inner mantle. Hence, the increased expression of CuZnSOD in the outer mantle of *T. squamosa* was probably a host's response to ameliorate oxidative stress related to photosynthesis in the symbionts, and not simply due to increased metabolic rate in the host cells. Evidently, the host clam must possess light- or O_2-responsive anti-oxidative defenses in order to align with the light-dependent photosynthetic activity of its symbionts.

Keywords: Symbiodiniaceae dinoflagellate, hyperoxia, oxidative stress, photosynthesis, reactive oxygen species, zooxanthellae

1. Introduction

Although tropical waters are deficient in nutrient and low in plankton content partly due to a lack of overturn (de Goeij et al., 2013), giant clams (family: Cardiidae, subfamily: Tridacninae) grow well in reef waters of the Indo-Pacific (Klumpp et al., 1992). This is because they possess symbiotic dinoflagellates (zooxanthellae) of the genera *Symbiodinium*, *Cladocopium*, *Durusdinium* and *Gerakladium*, singly or in various combinations and proportions as defined by the environmental conditions (Trench, 1987; LaJeunesse et al., 2018; Pochon et al., 2019; Guibert et al., 2020). These symbionts reside extracellularly inside a specialized tubular system (Norton et al., 1992) that originates from the host's digestive tract as a primary tube. The primary tube gives rise to many smaller secondary and tertiary tubules. While the tiny tertiary tubules permeate many organs, they are found mainly in the fleshy and colorful outer mantle, which is extensible for full exposure to light (Norton et al., 1992). The outer mantle is brightly colored, as it consists of iridophores that compose iridocytes containing stacks of tiny platelets (Griffiths et al., 1992). Iridocytes are located mainly in the upper 200 µm of the outer mantle and in very close proximity to the symbionts. Their platelets can scatter light of appropriate wavelengths to the symbionts while back-reflecting light of non-productive wavelengths (Holt et al., 2014; Ghoshal et al., 2016). Iridocytes can also absorb short-wavelength UV lights and remit them at longer wavelengths conducive for photosynthesis in the symbionts (Rossbach et al., 2020). In comparison, the inner mantle adjacent to the extrapallial fluid is thin and whitish, and plays an important role in shell formation (calcification). The host supplies symbiotic dinoflagellates with inorganic carbon, nitrogen and phosphorus to support their metabolism and growth (Furla et al., 2005). In return, symbionts share with the host photosynthates (Muscatine, 1990) that can fully satisfy the host's energy and nutritional needs (Fisher et al., 1985; Klumpp et al., 1992). Because of that, the fluted

giant clam, *Tridacna squamosa*, can survive and grow in Millipore-filtered seawater for more than 10 months with light as the sole energy source despite being deprived of access to planktonic/particulate matter (Fitt and Trench, 1981). It has been proposed that the supply of O_2 and photosynthates by the symbionts can boost the generation of ATP in the host to sustain the operation of Plasma Membrane Ca^{2+}-ATPase (PMCA) in the inner mantle during light-enhanced shell formation (Ip et al., 2017a).

Molecular O_2 is non-cytotoxic at its ground state. However, after gaining an extra electron, it can turn into a highly reactive superoxide radical, $O_2^{\bullet-}$, which is a type of reactive oxygen species (ROS; Scandalios, 1997). Many cellular reactions, including aerobic respiration and photosynthesis, generate $O_2^{\bullet-}$ as a by-product, and $O_2^{\bullet-}$ can in turn generate other ROS such as hydrogen peroxide, hydroxy radical and singlet oxygen (Perry et al., 2010). ROS, at controlled levels, participate in apoptosis, signaling, oxidative bursts in immune cells, as well as cell growth and adhesion (Boonstra and Post, 2004). However, imbalance between production and degradation of ROS could result in the accumulation of ROS leading to oxidative damage (Candas and Li, 2014). It has been established that ROS production can be augmented by high light intensity, UV radiation and extreme temperature (Scandalios, 2005), and accumulating ROS can damage DNA, proteins and lipids (Hermes-Lima 2004), and even alters the rate of senescence (Harman, 1956).

Cells can detoxify ROS enzymatically or by anti-oxidants (Birben et al., 2012). In particular, the enzyme superoxide dismutases (SODs; EC 1.15.1.1.) scavenge $O_2^{\bullet-}$, and dismutate two molecules of $O_2^{\bullet-}$ to H_2O_2. Then, H_2O_2 is detoxified to H_2O and O_2 catalyzed by glutathione peroxidase or catalase (Scandalios, 2005). The removal of $O_2^{\bullet-}$ prevents the formation of ROS and thus ameliorates the potential damage caused by excess ROS. SODs can be categorized into three classes, each with a specific catalytic metal ion and distinct peptides (Perry et al., 2010). Copper-

zinc superoxide dismutases (CuZnSODs) constitute one class of SODs that are predominantly cytoplasmic, although some are located in the compartment between the outer and inner mitochondrial membranes (Sturtz et al., 2001), while manganese superoxide dismutases (MnSODs) form another class of SODs that are generally located in the mitochondrial matrix of eukaryotes.

Animals and their tissues can be exposed to disparate levels of PO_2 under different physiological and/or environmental conditions. For instance, animals living in sunlit algal pools may encounter hyperoxia (atmospheric PO_2>21 kPa) when O_2 is enriched by algal photosynthesis. Animal tissues can also be confronted with high PO_2, when respiratory rate outpaces O_2 consumption. ROS production increases in insects exposed to pure O_2, (Beckman and Ames, 1998), resulting in the accumulation of carbonyl proteins (Sohal and Dubey, 1994) and the impairment of certain mitochondrial enzymes (Walker and Benzer, 2004). Cells cultured at high PO_2 also increase the generation of ROS, leading to genomic instability, DNA impairment, and senescence (Jagannathan et al., 2016). In comparison, giant clams are atypical as they possess extracellular symbiotic dinoflagellates that conduct photosynthesis and produce O_2 inside the animal's body during insolation. Because of that, hemolymph sampled from tissue sinuses of illuminated giant clams contains gas bubbles resulting from supersaturation of O_2 (Leggat et al., 1999). O_2 produced by the extracellular dinoflagellates would diffuse across the plasma membrane of host cells into their cytoplasm and lead to the formation of ROS therein. As the outer mantle of giant clams contains the highest density of symbionts (Norton et al., 1992; Poo et al., 2020), it would theoretically have the greatest needs to deal with possible oxidative damage. However, how the outer mantle ameliorates possible oxidative damage attributable to hyperoxia generated by photosynthesizing symbionts remains enigmatic at present.

Therefore, this study was undertaken to clone, sequence and characterize *CuZnSOD*/CuZnSOD from the colorful outer mantle of the fluted giant clam, *T. squamosa*, as we hypothesized that a cytosolic type of host SOD could be involved to deal with the ROS derived from hyperoxia generated by photosynthesized symbiotic dinoflagellates. *Tridacna squamosa* happens to be a deep water dwelling species, and its depth of occurrence ranges from 11 m to 20 m (Jantzen et al., 2008). Of note, Jantzen et al. (2008) exposed *T. squamosa* to a photosynthetic photon flux density (PPDF) of 128 ± 59 µmol photons m^{-2} s^{-1}, corresponding to the actual light intensity at ~20 m water depth, in their study, and Poo et al. (2020) also exposed *T. squamosa* to an underwater light intensity of 120 µmol photons m^{-2} s^{-1} to determine the phototrophic potential of dinoflagellates in five organs, including the extensible outer mantle. Hence, individuals of *T. squamosa* were exposed to an underwater PPDF of 120 µmol photons m^{-2} s^{-1} in this study. A molecular approach was adopted in this study because traditional enzymatic assays would not be able to differentiate the host SOD from the symbiont SOD, and it would be difficult to obtain pure host tissue extracts without contamination of dinoflagellates, particularly for the outer mantle. Based on molecular analyses, the identity of the sequenced CuZnSOD and its host origin were confirmed by phenogramic and sequence similarity analyses. Previous studies have demonstrated that the transcript and protein expression levels (Boo et al., 2019; Ca-Pharm et al., 2019b; Hiong et al., 2017b, 2018; Ip et al., 2017a, 2017b, 2018; Koh et al., 2018), or only the protein abundance (Boo et al. 2017; Cao-Pham, et al., 2019a: Chan et al., 2018, 2019; Chew et al., 2019; Hiong et al., 2017a; Poo et al., 2020) of many transporters are up-regulated in the ctenidium, outer mantle and inner mantle of *T. squamosa* in response to illumination, in order to align with photosynthetic activities in the symbiotic dinoflagellates. Therefore, efforts were made to examine transcript levels and protein abundance of *CuZnSOD*/CuZnSOD in the outer mantle and inner mantle in

response to 3, 6 or 12 h of light exposure as compared with controls kept in darkness for 12 h. The hypothesis tested was that light exposure and/or the consequential hyperoxic stress would upregulate the expression levels of *CuZnSOD*/CuZnSOD in the outer mantle, but not the inner mantle, of *T. squamosa*.

2. Materials and methods

2.1. Giant clams

Individuals of *T. squamosa* (521 ± 184 g, inclusive of shell valves; *N*=16) were procured from Xanh Tuoi Tropical Fish Co. of Vietnam, and kept in three separate tanks. Each tank had a dimension of L90 cm x W62 cm x H60 cm and contained 335 L of recirculating seawater. The water conditions were as follows: temperature, ~26°C; pH, 8.1-8.3; salinity, 30-32; hardness, 143–179 ppm; calcium, 380–420 ppm; total ammonia, <0.25 ppm; nitrate, 0 ppm; phosphate, <0.25 ppm. Each tank was illuminated with two sets of Aquazonic T5 lighting systems (Yi Hu Fish Farm Trading, Singapore), each containing four 40 W fluorescence tubes (90 cm; 2x Sun tubes and 2x Actinic blue tubes), from the top. The shaded light intensity (PPDF) measured in water at the level of the giant clams was 120 μmol photons m^{-2} s^{-1} (400-700 nm), which is equivalent to the intensity adopted by Jantzen et al. (2008) for *T. squamosa*. Light intensity was measured by a Skye SKP 200 display meter connected with a SKP 215 PAR Quantum sensor (Skye Instruments Ltd, UK). Although it would be ideal to expose giant clams individually to the experimental conditions, individuals were sampled directly and randomly from the three glass tanks due to the limitation of re-circulating tanks available and the need to keep them in the exact conditions (including salinity, water quality, and light intensity). Research on giant clams was exempted from approval by the Nanyang Technological University Institutional Animal Care and Use Committee.

2.2. Experimental conditions and tissue sampling

Four individuals were sampled at the end of the 12 h dark period of the 12 h light:12 h dark regime (*N*=4; control). Another twelve individuals were sampled at 3, 6, or 12 h after exposure to light (*N*=4 for each time point). Parallel controls with individuals exposed to 24 h of darkness were avoided as it was important to simulate the normal dark/light hours experienced by the giant clams

in their natural habitat. Giant clams were anaesthetized with 0.2% phenoxyethanol, and then forced open to cut the adductor before sampling the outer mantle, inner mantle, ctenidium, foot muscle, byssal retractor muscle, heart, hepatopancreas and kidney. Tissue samples were immediately freeze-clamped in liquid nitrogen and stored at -80°C until analysis.

2.3. Extraction of RNA and synthesis of cDNA

RNA was extracted from tissue samples using TRI Reagent® (Sigma-Aldrich Co., St. Louis, MO, USA), and the extracted total RNA were further purified using the RNeasy Plus Mini Kit (Qiagen GmbH, Hilden, Germany) following the manufacturers' protocol. A Shimadzu BioSpec-nano spectrophotometer (Shimadzu Corporation, Kyoto, Japan) was used to determine the RNA concentration, while the integrity of RNA was checked by electrophoresis. RNA was converted to cDNA using a RevertAid™ cDNA synthesis kit (Thermo Fisher Scientific Inc., Waltham, MA, USA).

2.4. PCR, cloning and RACE PCR

A set of primers (forward: 5′-GCWGTYTGTGTVTTGAARGG-3′; reverse: 5′-CCAATSACWCCACAAGCCARACG-3′) was designed at conserved regions based on the alignment of *Crassostrea madrasensis CuZnSOD* (JX532084.1), *Mytilus edulis CuZnSOD* (AJ581746.1), *Mytilus galloprovincialis CuZnSOD* (FM177867.1), *Ostrea edulis CuZnSOD* (GU320695.1) and *Pinctada fucata CuZnSOD* (JX013537.3). PCR was performed using this pair of primers and DreamTaq™ polymerase (Thermo Fisher Scientific Inc.) in a 9902 Veriti 96-well thermal cycler (Applied Biosystems, Carlsbad, CA) to obtain a partial *CuZnSOD* sequence from the outer mantle of *T. squamosa*. The PCR cycling conditions were 94°C for 3 min, followed by 34 cycles of 94°C for 30 s, 50°C for 30 s, 72°C for 1 min and 1 cycle of final extension at 72°C for 10 min. Thereafter, cloning experiments were performed as previously described in Hiong et

196 al. (2017a), which indicated the presence of only one major form of *CuZnSOD* fragments. The
197 complete coding sequence of this major form of *CuZnSOD* was obtained by using a SMARTer
198 RACE cDNA amplification kit (Clontech Laboratories, Mountain View, CA, USA). The primers
199 for 5' and 3' RACE were 5′-TCCCAGGTCACCAACATGCCTAATTTCA-3′ and 5′-
200 AGGCATGTTGGTGACCTGGGAAATGTG-3′, respectively. Samples were prepared for
201 sequencing using the BigDye Terminator v3.1 Cycle Sequencing Kit (Thermo Fisher Scientific
202 Inc.), and sequencing was performed using an automated 3130XL Genetic Analyzer (Thermo
203 Fisher Scientific Inc.). BioEdit version 7.2.5 (Hall, 1999) was used to analyze the sequences
204 obtained. The complete coding cDNA sequence of *CuZnSOD* obtained from the outer mantle of
205 *T. squamosa* has been deposited into GenBank (accession number: MT019278).

206 ***2.5. Expression of CuZnSOD in various organs/tissues***

207 Based on the *CuZnSOD* sequence obtained from the outer mantle of *T. squamosa*, a pair of
208 gene-specific primers (forward: 5'- CTGTTTGTGTCCTGAAAGGTC -3' and reverse: 5'-
209 AATGCCAATCACACCACAC -3') was designed to examine the gene expression of *CuZnSOD*
210 in the outer mantle, inner mantle, ctenidium, foot muscle, byssal retractor muscle, heart,
211 hepatopancreas and kidney using PCR. The PCR was performed as mentioned in section 2.4. The
212 resulting PCR products were examined by agarose gel (1%) electrophoresis.

213 ***2.6. Deduced amino acid sequence and phenogramic analysis***

214 The *CuZnSOD* nucleotide sequence obtained from *T. squamosa* was translated into the
215 CuZnSOD amino acid sequence using the ExPASy Proteomic server
216 (http://web.expasy.org/translate/). The deduced CuZnSOD amino acid sequence was aligned with
217 other CuZnSOD sequences from various animals. A phenogramic analysis on the CuZnSOD
218 sequence of *T. squamosa* together with those from molluscs and algae (obtained from GenBank)

was conducted using the Phylip programme and the neighbor-joining method with 1000 bootstrap replicates (Felsentein, 1989), in order to verify the host origin of the CuZnSOD obtained.

2.7. Quantitative real-time PCR (qPCR)

qPCR analysis was performed on samples obtained from the outer mantle and inner mantle. The reaction for each sample was conducted in triplicates using a StepOnePlus™ Real-Time PCR System (Applied Biosystems) with specific *CuZnSOD* qPCR primers designed according to the sequence obtained from *T. squamosa* (forward: 5'-CACTAACAGGAGCACATTCCA-3'; reverse: 5'-AATGCCAATCACACCACAC-3'). The amplification efficiency of the *CuZnSOD* primers was 99.8%. The qPCR reactions and the cycling conditions were based on the methods of Hiong et al. (2017a, 2017b). The presence of only one PCR product without non-specific amplification was ascertained by analyzing the melt curve. Using plasmids that contained a pure amplicon of the region of *CuZnSOD* defined by the set of qPCR primers, a standard curve was constructed for the absolute quantification of *CuZnSOD* transcripts in the samples. The quantity of *CuZnSOD* transcripts in a sample was expressed as copy of transcripts per ng of total RNA.

2.8. SDS-PAGE electrophoresis and Western blotting

Based on the epitope sequence of ADVDDLGKGGHELS designed for CuZnSOD of *T. squamosa*, a rabbit polyclonal anti-CuZnSOD antibody was custom-made by GenScript (Piscataway, NJ, USA). Protein extraction, SDS-PAGE electrophoresis and Western blotting were performed following the procedures of Hiong et al. (2017a, 2017b). The blots were scanned at 600 dpi resolution using a flatbed scanner (CanoScan 9000F Mark II, Canon USA Inc., NY, USA). The scanned image was analyzed for band optical density by ImageJ (version 1.50, NIH) against a 21 step transmission scanner scale (1" x 5.5"; Tiffen #EK1523406T) as reference. The arbitrary optical density of CuZnSOD normalized with that of α-tubulin was used to express the protein

abundance of CuZnSOD. A peptide competition assay was performed following the methods of Hiong et al. (2017a, 2017b) to confirm the specificity of the anti-CuZnSOD antibody.

2.9. Statistical analysis

Results were presented as means ± the standard error of the mean (S.E.M.). Levene's test was used to check for the difference among variances. Differences among means were evaluated by one-way analysis of variance (ANOVA), followed by Tukey's test if the variance was equal or Dunnett's T3 test if the variance was unequal. Results were regarded as statistically significant when P is less than 0.05. All statistical analyses were performed using the SPSS Statistics version 20 software (IBM Corporation, Armonk, NY, USA).

3. Results

3.1. Nucleotide and translated amino acid sequences

There were a total of 462 bp in the complete cDNA coding sequence of *CuZnSOD* obtained from the outer mantle of *T. squamosa*. This nucleotide sequence would encode a CuZnSOD sequence of 154 amino acids (Fig. 1) with an estimated molecular mass of 15.6 kDa. The deduced CuZnSOD amino acid sequence contained the four histidine residues (His47, His49, His64 and His121) that coordinate the catalytic Cu^{2+} (Fig. 1). The residues that contribute to the binding of Zn^{2+} (His64, His72, His81 and Asp84; Fig. 1), and the residue that is involved in gatekeeping (Arg144), were also present in CuZnSOD of *T. squamosa* (Fig. 1). Additionally, CuZnSOD of *T. squamosa* consisted of Cys58 and Cys147, which are known to form disulfide bonds that stabilize the entire structure. The two CuZnSOD signatures, namely FHVHQYGDN from positions 46 to 54 and GNAGGRLACG from positions 139 to 148, were mostly conserved in CuZnSOD of *T. squamosa* (Fig. 1).

3.2. Phenogramic analyses

Phenogramic analysis revealed that CuZnSOD of *T. squamosa* was grouped together with CuZnSOD of animal origin like molluscs and flies, and separated from CuZnSOD of algal origin (Fig. 2). As *T. squamosa* is a bivalve, its CuZnSOD had the highest sequence similarity with molluscan CuZnSODs from the Class, Bivalvia, rather than from the Class, Gastropoda or the Class, Cephalopoda (Table 1). Additionally, its CuZnSOD had the lowest similarity with algal CuZnSOD (Table 1). Taken together, these results denoted the host-origin of the sequence of CuZnSOD obtained from *T. squamosa*.

3.3. Gene expression in various tissues

CuZnSOD expression was detected in all organs and tissues of *T. squamosa* examined (Fig. 3). The bands obtained for outer mantle, ctenidium, hepatopancreas and kidney displayed were more intense than those obtained for the inner mantle, foot muscle, byssal muscle and heart (Fig. 3).

3.4. Effects of light exposure on transcript levels and protein abundance of CuZnSOD/CuZnSOD *in the outer mantle and inner mantle*

In the outer mantle of *T. squamosa*, the transcript levels of *CuZnSOD* remained unchanged during 12 h of light exposure as compared with the control kept in darkness for 12 h (Fig. 4a), but the protein abundance of CuZnSOD increased significantly (~2.3-fold) after 12 h of light exposure (Fig. 5), indicating that the regulation of expression is at the translational level. By contrast, light exposure had no significant effects on the transcript level (Fig. 4b) and protein abundance (Fig. 6) of *CuZnSOD*/CuZnSOD in the inner mantle of *T. squamosa*.

4. Discussion

Although the extensible outer mantle of giant clams can be exposed directly and fully to light, symbiotic dinoflagellates residing therein are shaded by several layers of host cells and would therefore receive only a portion of the irradiance (Holt et al., 2014). In order to support photosynthesis in the symbionts, the outer mantle uniquely possesses iridocytes that forward-scatter light of appropriate wavelengths to them, but even then, only a small fraction (~5-10%) of the incident light would reach the symbionts present in the outer mantle (Holt et al., 2014). Presumably, symbiotic dinoflagellates residing in tissues located inside the mantle cavity and lacking iridocytes would receive negligible irradiance. Yet, Poo et al. (2020) have recently reported the presence of symbionts in four organs (inner mantle, ctenidium, hepatopancreas and foot muscle) of *T. squamosa*, which are devoid of iridocytes and do not have direct exposure to light. Particularly, symbiotic dinoflagellates are present at relatively high densities in specific regions of the inner mantle and the foot muscle (Poo et al., 2020). In the inner mantle, a peculiar area adjacent to the hinge of the shell-valves contains substantial quantities of symbionts and is therefore brownish in color. Although the outer mantle of *T. squamosa* has the greatest phototrophic potential as reflected by its high transcript level of *T. squamosa* zooxanthellal form II *ribulose-1,5-bisphosphate carboxylase/oxygenase* (*TSZrbcII*), a moderate level of *TSZrbcII* transcripts is also detected in the inner mantle despite the lack of iridocytes (Poo et al., 2020). Furthermore, the protein expression level of TSZRBCII in the outer mantle, but not that in the inner mantle, can be enhanced by illumination. Therefore, it can be concluded that the inner mantle has low phototrophic potential, and the symbionts residing therein may serve some non-phototrophic functions, like nitrogen metabolism including amino acid synthesis (Ip et al., 2020b), to benefit the host. As a corollary, it can be postulated that the outer mantle, but not the inner

mantle, would need to augment the defense against hyperoxia-related ROS caused by phototrophic activities in the symbionts during illumination. Indeed, results obtained from this study support such a postulate.

4.1. Properties of the host CuZnSOD of T. squamosa

Based on sequence similarity and phenogramic analyses, it can be concluded that the sequence of CuZnSOD obtained from *T. squamosa* is derived from the host clam. In eukaryotes, CuZnSOD exists as homodimers, with each subunit having an active site for one Cu^{2+} and one Zn^{2+} (Culotta et al., 2006). Cu^{2+} is the main catalytic ion in CuZnSOD which participates in the ping-pong redox mechanism with $O_2^{\bullet-}$ (Valentine et al., 2005), and is bound by the nitrogen atoms of four histidine residues, all of which have been conserved in the CuZnSOD of *T. squamosa* (His47, His49, His64 and His121; Culotta et al., 2006). Although Zn^{2+} is not essential to the dismutation reaction catalysed by CuZnSOD, its binding gives the enzyme extra thermal stability (Furukawa et al., 2004). The residues that aid in the association of Zn^{2+} to CuZnSOD are also highly conserved (His64, His72, His81 and Asp84; Culotta et al., 2006). In addition, CuZnSOD of *T. squamosa* contains two conserved cysteine residues, Cys58 and Cys147, which are involved in the formation of an intramolecular disulfide bond (Sheng et al., 2014). This disulfide bond stabilizes the Loop IV structure of CuZnSOD, which plays an important role in the dimerization of the enzyme (Culotta et al., 2006). The conserved Arg144 acts as a gatekeeping residue to the active site to regulate the access of $O_2^{\bullet-}$ to the metal binding sites, and has also been demonstrated to be a catalytically important residue (Sheng et al., 2014). Overall, CuZnSOD of *T. squamosa* contains all the important residues for the catalytic activity and stability of the enzyme, as well as the two family signatures (FHVHQYGDN from positions 46 to 54 and GNAGGRLACG from positions 139 to 148) of CuZnSOD.

At first glance, the gene expression of *CuZnSOD* in various tissues/organs of *T. squamosa* kept in darkness for 12 h (control) has no correlation with the density of the symbiotic dinoflagellates present, as the expression of *CuZnSOD* in the outer mantle was not substantially different from those in other organs. However, it would be important to elucidate whether the expression of *CuZnSOD*/CuZnSOD in the outer mantle could be enhanced by illumination, and whether the inner mantle would display a similar response to light.

4.2. Light exposure augments the protein abundance of CuZnSOD *in the outer mantle*

We report for the first time that there was a significant increase in the protein abundance of CuZnSOD in the outer mantle of *T. squamosa* after 12 h of light exposure. It can be inferred that the increase had occurred between hour 6 and hour 12, because time was needed for the protein abundance of CuZnSOD to achieve a ~2.3-fold increase from the control level. As light exposure had no significant effect on the transcript level of *CuZnSOD* in the outer mantle, the regulation of expression is apparently set at the translational level. Translational regulation would circumvent energetic requirements of transcriptional regulation related to synthesis, processing and exporting of mRNA, and allow for a faster response to external changes (Lackner and Bähler, 2008). Furthermore, it is logical to deduce that the increase in protein abundance of CuZnSOD would result in a higher capacity to detoxify SOD in the outer mantle of *T. squamosa* during illumination.

Light-driven energy transfer through electron transport is associated with ROS formation. Photosynthesis is a well-established source ROS in phototrophic organisms (Foyer, 2018), and photosynthesizing symbiotic dinoflagellates would increase ROS production during illumination. In giant clams, ROS generated by symbionts are unlikely to have a direct impact on the oxidative status of the host cells in the outer mantle because symbionts are located extracellularly inside the lumen of the tertiary zooxanthellal tubules. However, in light, photosynthesizing symbiotic

dinoflagellates generate large amounts of O_2 and release it directly into the tubular fluid and hemolymph of the host. It is probable that O_2 diffuses across plasma membranes of host cells, and subsequently combines with the electrons that leak out from the host's mitochondrial electron transport chain to form $O_2^{\bullet-}$ within the cytoplasm (Bandyopadhyay et al., 1999). Therefore, the elevated levels of the host's CuZnSOD could function to mitigate oxidative damage by detoxifying $O_2^{\bullet-}$ in the cytosol.

Recently, Hiong et al. (2018) have obtained the complete cDNA coding sequence of a host's *MnSOD* from the outer mantle of *T. squamosa*, and demonstrated that its gene and protein expression levels could also be upregulated during light exposure. In light, there could be increases in the metabolic rate and mitochondrial ROS production in host's cells of the outer mantle. This is because they need to increase the supply of nutrients to and the absorption of photosynthates from the symbionts. Hence, in the outer mantle of *T. squamosa*, transcript and protein expression levels of mitochondrial *MnSOD*/MnSOD need to be upregulated to detoxify excess mitochondrial $O_2^{\bullet-}$ attributable to increases in the host's metabolic rate in order to prevent oxidative damage. As a fraction of CuZnSOD and its chaperone protein are known to be localized in the space between the inner and outer mitochondrial membranes (Sturtz et al., 2001), it could help to remove $O_2^{\bullet-}$ that has leaked out of the mitochondrial matrix into the intermembrane space (Finkel, 2011) and thus prevent the escape of mitochondrial ROS from the intermembrane space into the cytosol.

*4.3. The transcript and protein expression levels of CuZnSOD/*CuZnSOD *remain unchanged in the inner mantle during light exposure*

The rate of shell formation in giant clams is known to be higher in light than in darkness (Rossbach et al., 2019), and the inner mantle is involved directly in shell formation. In fact, it has been reported that the gene and/or protein expression levels of PMCA (Ip et al., 2018), Na^+/Ca^{2+}

exchanger 3 homolog (Boo et al., 2019), Na^+/K^+-ATPase α-subunit (Boo et al., 2018), beta-Na^+/H^+ exchanger homolog (Cao-Pham et al., 2019a), carbonic anhydrase 4 homolog (Chew et al., 2019) and carbonic anhydrase 2 homolog (Ip et al., 2017b) are upregulated in the inner mantle of *T. squamosa* during illumination to enhance the transport of Ca^{2+}, HCO_3^- and H^+ in support of light-enhanced shell formation. Therefore, it is logical to deduce that the metabolic rate of host cells in the inner mantle should be higher in light than in darkness. However, the transcript and protein expression levels of *CuZnSOD*/CuZnSOD remained unchanged in the inner mantle of *T. squamosa* during 12 h of illumination. Notably, the major difference between the inner mantle and the outer mantle is that the former has many fewer symbiotic dinoflagellates, lower phototrophic potential and no iridophores as compared with the latter (Poo et al., 2020). Together, these results denote the increased expression of *CuZnSOD*/CuZnSOD in the outer mantle of *T. squamosa* during light exposure as a response to oxidative stresses related to photosynthetic activities of the symbionts and not simply to increases in the metabolic rate of the host clam.

4.4. Unusual light-dependent expression of CuZnSOD in the outer mantle of T. squamosa

Plants possess photoreceptors and can therefore respond to light. They can also respond to light via signals generated by circadian rhythm or derived from the photosynthetic electron transport chain (Pfannschmidt et al., 2001). For instance, the transcript levels of genes related to photosynthesis display diurnal changes (Harmer et al., 2000; Blasing et al., 2005). Particularly, the transcript levels of *CuZnSOD* increase in tomato (Perl-Treves and Galun 1991) and *Arabidopsis* (Kliebenstein et al., 1998; Xing et al., 2013) during light exposure. By contrast, the transcript and protein expression levels of *CuZnSOD*/CuZnSOD in non-symbiotic animal are not affected by illumination. Yet, light exposure led to a significant increase in the protein abundance of the host CuZnSOD in the outer mantle of *T. squamosa*. At present, it is uncertain whether such an increase

in expression was resulted directly from light-responsive regulatory mechanisms of the host or from ROS produced by the host due to hyperoxia generated by the photosynthesizing symbiotic dinoflagellates during illumination.

Notably, *T. squamosa* possesses many host's enzymes and transporters that display light-enhanced gene and protein expression, and, unlike the host CuZnSOD, many of them are not known to respond to ROS and O_2. Hence, it is probable that the host has developed a light-response signaling mechanism to coordinate the gene and protein expression levels of protein catalysts involved in a wide range of light-dependent physiological processes. These light-enhanced processes include shell formation (Ip et al., 2017a, 2018; Boo et al., 2017, 2019), H^+ excretion (Ip et al., 2015; Hiong et al., 2017b; Ip et al., 2018; Cao-Pham et al., 2019a), Ca^{2+} absorption (Cao-Pham et al., 2019b), inorganic carbon absorption and transport (Ip et al., 2017b; Koh et al., 2018; Chew et al., 2019), ammonia absorption and assimilation (Hiong et al., 2017a; Boo et al., 2018), and absorption of urea (Chan et al., 2018, 2019), nitrate (Ip et al., 2020a), phosphate (Chan et al., 2020) as well as glucose (Chan et al., 2019). Therefore, it is also possible that the anti-oxidative defense enzymes (MnSOD, Hiong et al., 2018; CuZnSOD, this study) of *T. squamosa* are also regulated by the same host-mediated light-responsive signaling mechanism. After all, the host clam must possess light-responsive processes; only then, will it be able to support and complement, as well as to ameliorate the oxidative stress arising from, the light-dependent photosynthetic activity in its symbionts residing in the outer mantle.

The oxidative stress hypothesis of aging states that organismal aging occurs because of accumulative oxidative damage of important cellular macromolecules and organelles caused by ROS generated from aerobic respiration (Harman, 1972). Nonetheless, despite living in symbiosis with phototrophic dinoflagellates that generate O_2 inside their bodies, giant clams have exceptional

longevity. For instance, the smooth giant clam, *Tridacna derasa*, has a maximum lifespan of >100 years, while the bay scallop, *Argopecten irradians*, can live only up to 2 years. Yet, the basal anti-oxidative capacity together with the activities of SODs and catalase in *T. derasa* are comparable to those in *A. irradians* (Ungvari et al., 2012). Hence, as demonstrated by CuZnSOD (this study) and MnSOD (Hiong et al., 2018) of *T. squamosa*, the key factor to the extraordinary success of giant clams in detoxifying ROS may lie in the novel light-inducible nature of their anti-oxidative enzymes rather than the constant expression of these enzymes at elevated levels under all conditions.

4.5. Perspective

Various environmental perturbations and stressors, particularly high temperature and high irradiance, can generate a stress response called 'bleaching' in symbiotic reef organisms. Bleaching eventually results in the loss of symbiotic dinoflagellates and/or their photosynthetic pigments from the host (Glynn and D'croz, 1990; Lesser et al., 1990). In scleractinian corals, the detrimental bleaching process is attributable to the overproduction of ROS by symbiotic dinoflagellates generated by their damaged photosynthetic apparatus (Lesser, 1996; Downs et al., 2002), although there is evidence against such a proposition (Nielsen et al., 2018). Notably, coral bleaching can occur in the absence of light, suggesting that damage to photosynthetic machinery may not be necessarily involved (Tolleter et al., 2013). As symbionts are located intracellularly inside symbiosomes in scleractinian corals, the leakage of ROS from the intracellular symbionts could overwhelm the host's oxidative defense system and cause direct damage to the coral cells (Lesser et al., 1990; Down et al., 2002). Bleaching can also occur in giant clams under certain environmental conditions, leading to a reduction in the population of symbiotic dinoflagellates and discoloration of the outer mantle (Addessi, 2001; Leggat et al., 2003). However, unlike

448 scleractinian corals, giant clams harbor symbiotic dinoflagellates extracellularly inside a tubular
449 system, and these symbionts are surrounded by the tubular fluid. Therefore, the oxidative theory
450 of coral bleaching may not be directly relevant to the bleaching process in giant clams. Results
451 from this study revealed that the light-enhanced expression of *CuZnSOD*/CuZnSOD in the outer
452 mantle of *T. squamosa* could be a host's response to ameliorate hyperoxic oxidative stress related
453 to photosynthesis in the symbionts. However, the possibility of *T. squamosa* being able to change
454 the expression levels of *CuZnSOD*/CuZnSOD, and perhaps also those of other anti-oxidative
455 enzymes, in response to high environmental temperature and/or high irradiance cannot be ignored.
456 Hence, efforts should be made in the future to examine the effects of environmental stressors on
457 the host's oxidative defense mechanisms in *T. squamosa* in order to evaluate whether they play a
458 role in the bleaching process in giant clams.
459

460 **References**

461 **References**

462 Addessi, L., 2001. Giant clam bleaching in the lagoon of Takapoto atoll (French Polynesia). Coral
463 Reefs 19, 220. https://doi.org/10.1007/PL00006957.

464 Bandyopadhyay, U., Das, D., Banerjee, R.K., 1999. Reactive oxygen species: Oxidative damage
465 and pathogenesis. Curr. Sci. 77, 658–666.

466 Beckman, K.B., Ames, B.N. 1998. The free radical theory of aging matures. Physiol. Rev. 78,
467 547–581.

468 Birben, E., Sahiner, U.M., Sackesen, C., Erzurum, S., Kalayci, O., 2012. Oxidative stress and
469 antioxidant defense. World Allergy Organ J. 5, 9–19.
470 https://doi.org/10.1097/WOX.0b013e3182439613.

471 Blasing, O.E., Gibon, Y., Gunther, M., Hohne, M., Morcuende, R., Osuna, D., Thimm, O., Usadel,
472 B., Scheible, W.R., Stitt, M., 2005. Sugars and circadian regulation make major
473 contributions to the global regulation of diurnal gene expression in *Arabidopsis*. Plant Cell
474 17, 3257–3281. https://doi.org/10.1105/tpc.105.035261.

475 Boo, M.V., Hiong, K.C., Choo, C.Y.L., Cao-Pham, A.H., Wong, W.P., Chew, S.F., Ip, Y.K., 2017.
476 The inner mantle of the giant clam, *Tridacna squamosa*, expresses a basolateral Na^+/K^+-
477 ATPase α-subunit, which displays light-dependent gene and protein expression along the
478 shell-facing epithelium. PLoS ONE 12 (10), e0186865.
479 https://doi.org/10.1371/journal.pone.0186865.

480 Boo, M.V., Hiong, K.C., Goh, E.J.K., Choo, C.Y.L., Wong, W.P., Chew, S.F., Ip, Y.K., 2018. The
481 ctenidium of the giant clam, *Tridacna squamosa*, expresses an ammonium transporter 1
482 that displays light-suppressed gene and protein expression and may be involved in
483 ammonia excretion. J. Comp. Physiol. B 188, 765–777. https://doi.org/10.1007/s00360-
484 018-1161-6.

485 Boo, M.V., Hiong, K.C., Wong, W.P., Chew, S.F., Ip, Y.K., 2019. Shell formation in the giant
486 clam, *Tridacna squamosa*, may involve an apical Na^+/Ca^{2+} Exchanger 3 homolog in the
487 shell-facing epithelium of the whitish inner mantle, which displays light-enhanced gene
488 and protein expression. Coral Reefs 38, 1173–1186. https://doi.org/10.1007/s00338-019-
489 01848-y.

490 Boonstra, J., Post, J.A., 2004. Molecular events associated with reactive oxygen species and cell
491 cycle progression in mammalian cells. Gene 337, 1–13.
492 https://doi.org/10.1016/j.gene.2004.04.032.

493 Candas, D., Li, J.J., 2014. MnSOD in oxidative stress response-potential regulation via
494 mitochondrial protein influx. Antioxid. Redox Signal. 20, 1599–1617.
495 https://doi.org/10.1089/ars.2013.5305

496 Cao-Pham, A.H., Hiong, K.C., Boo, M.V., Choo, C.Y.L., Pang, C.Z., Wong, W.P., Neo, M.L.,
497 Chew, S.F., Ip, Y.K., 2019a. Molecular characterization, cellular localization, and light-
498 enhanced expression of Beta-Na^+/H^+ Exchanger-like in the whitish inner mantle of the

giant clam, *Tridacna squamosa*, denote its role in light-enhanced shell formation. Gene 695, 101–112. https://doi.org/10.1016/j.gene.2019.02.009.

Cao-Pham, A.H., Hiong, K.C., Boo, M.V., Choo, C.Y.L., Wong, W.P., Chew, S.F., Ip, Y.K., 2019b. Calcium absorption in the fluted giant clam, *Tridacna squamosa*, may involve a homolog of Voltage-gated Calcium Channel subunit α1 that has an apical localization and displays light-enhanced protein expression in the ctenidium. J. Comp. Physiol. B 189, 693–706. https://doi.org/10.1007/s00360-019-01238-4.

Chan, C.Y.L., Hiong, K.C., Boo, M.V., Choo, C.Y.L., Wong, W.P., Chew, S.F., Ip, Y.K., 2018. Light exposure enhances urea absorption in the fluted giant clam, *Tridacna squamosa*, and up-regulates the protein abundance of a light-dependent urea active transporter, DUR3-like, in its ctenidium. J. Exp. Biol. 221, jeb176313. doi:10.1242/jeb.176313.

Chan, C.Y.L, Hiong, K.C., Choo, C.Y.L., Boo, M.V., Wong, W.P., Chew, S.F., Ip, Y.K., 2019. Illuminated fluted giant clams, *Tridacna squamosa*, upregulate protein abundance of an apical Na^+:Glucose Cotransporter 1 homolog in the ctenidium, and increase exogenous glucose absorption that can be impeded by urea. J. Exp. Biol. 222, jeb195644. doi:10.1242/jeb.195644.

Chan, C.Y.L., Hiong, K.C., Choo, C.Y.L., Boo, M.V., Wong, W.P., Chew, S.F., Ip, Y.K., 2020. Light-enhanced phosphate absorption in the fluted giant clam, *Tridacna squamosa*, entails an increase in the expression of sodium-dependent phosphate transporter 2a in its colorful outer mantle. Coral Reefs https://doi.org/10.1007/s00338-020-01930-w

Chew, S.F., Koh, C.Z.Y., Hiong, K.C., Choo, C.Y.L., Wong, W.P., Neo, M.L., Ip, Y.K., 2019. Light-enhanced expression of Carbonic Anhydrase 4-like supports shell formation in the fluted giant clam *Tridacna squamosa*. Gene 683, 101–112. https://doi.org/10.1016/j.gene.2018.10.023.

Culotta, V.C., Yang, M., O'Halloran, T.V., 2006. Activation of superoxide dismutases: Putting the medal to the pedal. Biochim. Biophys. Acta, Mol. Cell Res. 1763, 747–758. https://doi.org/10.1016/j.bbamcr.2006.05.003.

De Goeij, J.M., Van Oevelen, D., Vermeij, M.J., Osinga, R., Middelburg, J.J., de Goeij, A.F., Admiraal, W., 2013. Surviving in a marine desert: the sponge loop retains resources within coral reefs. Science 342, 108–110.

Downs, C.A., Fauth, J.E., Halas, J.C., Dustan, P., Bemiss, J., Woodley, C.M., 2002. Oxidative stress and seasonal coral bleaching. Free Radic. Biol. Med. 33, 533–543.

Felsentein, J., 1989. PHYLIP–Phylogeny Inference Package (Version 3.2). Cladistics 5, 164–166.

Finkel, T., 2011. Signal transduction by reactive oxygen species. J. Biol. Chem. 194, 7-15.

Fisher, C.R., Fitt, W.K., Trench. R.K., 1985. Photosynthesis and respiration in *Tridacna gigas* as a function of irradiance and size. Biol. Bull. 169, 230–245.

Fitt, W.K., Trench, R.K., 1981. Spawning, development and acquisition of zooxanthellae by *Tridacna squamosa* (Mollusca, Bivalvia). Biol. Bull. 161, 213–235.

Foyer, C.H., 2018. Reactive oxygen species, oxidative signaling and the regulation of photosynthesis. Environ. Exp. Botany 154, 134–142.

539 Furla, P., Allemand, D., Shick, J.M., Ferrier-Pagès, C., Richier, S., Plantivaux, A., Merle, P.,
540 Tambutté, S., 2005. The symbiotic anthozoan: a physiological chimera between alga and
541 animal. Integr. Comp. Biol. 45, 595–604.

542 Furukawa, Y., Torres, A.S., O'Halloran, T.V., 2004. Oxygen-induced maturation of SOD1: a key
543 role for disulfide formation by the copper chaperone CCS. EMBO J. 23, 2872–2881.

544 Ghoshal, A., Eck, E., Gordon, M., Morse, D.E., 2016. Wavelength-specific forward scattering of
545 light by Bragg-reflective iridocytes in giant clams. J. R. Soc. Interface 13:20160285.
546 https://doi.org/10.1098/rsif.2016.0285.

547 Glynn, P.W., D'Croz, L., 1990. Experimental evidence for high temperature stress as the cause of
548 El Nino-coincident coral mortality. Coral Reefs 8, 181–191.
549 https://doi.org/10.1007/BF00265009.

550 Griffiths, D.J., Winsor, H., Luongvan, T., 1992. Iridophores in the mantle of giant clams. Aust. J.
551 Zool. 40, 319–326.

552 Guibert, I., Lecellier, G., Torda, G., Ponchon, X., Berteaux-Lecellier, V. 2020.Metabarcoding
553 reveals distinct microbiotypes in the giant clam *Tridacna maxima*. Micobiome 8:57
554 https://doi.org/10.1186/s40168-020-00835-8

555 Hall, T.A., 1999. BioEdit: a user-friendly biological sequence editor and analysis program for
556 Windows 95/98/NT. Nucleic Acids Symp. Ser. 41, 95–98.

557 Harman, D., 1956. Aging: a theory based on free radical and radiation chemistry. J. Gerontol. 11,
558 298–300. https://doi.org/10.1093/geronj/11.3.298.

559 Harman, D., 1972. The biologic clock: the mitochondria? J. Am. Geriatr. Soc. 20, 145–147.
560 https://doi.org/10.1111/j.1532-5415.1972.tb00787.x.

561 Harmer, S.L., Hogenesch, L.B., Straume, M., Chang, H.S., Han, B., Zhu, T., Wang, X., Kreps,
562 J.A., Kay, S.A., 2000. Orchestrated transcription of key pathways in Arabidopsis by the
563 circadian clock. Science 290, 2110–2113.

564 Hermes-Lima, M., 2004. Oxygen in biology and biochemistry: role of free radicals. In: Storey,
565 K.B. (Ed.), Functional metabolism: regulation, and adaptation. John Wiley & Sons Inc.,
566 Hoboken, NJ, pp. 319–368.

567 Hiong, K.C., Cao-Pham, A.H., Choo, C.Y.L., Boo, M.V., Wong, W.P., Chew, S.F., Ip, Y.K., 2017a.
568 Light-dependent expression of a Na^+/H^+ exchanger 3-like transporter in the ctenidium of
569 the giant clam, *Tridacna squamosa*, can be related to increased H^+ excretion during light-
570 enhanced calcification. Physiol. Rep. 5(8), e13209. https://doi.org/10.14814/phy2.13209.

571 Hiong, K.C., Choo, C.Y.L., Boo, M.V., Ching, B., Wong, W.P., Chew, S.F., Ip, Y.K., 2017b. A
572 light-dependent ammonia-assimilating mechanism in the ctenidia of a giant clam. Coral
573 Reefs 36, 311–323. https://doi.org/10.1007/s00338-016-1502-4.

574 Hiong, K.C., Koh, C.Z.Y., Boo, M.V., Choo, C.Y.L., Wong, W.P., Chew, S.F., Ip, Y.K., 2018.
575 The colorful mantle of the giant clam, *Tridacna squamosa*, expresses a light-dependent
576 manganese superoxide dismutase to ameliorate oxidative stresses due to its symbiotic
577 association with zooxanthellae. Coral Reefs 37, 1039–1051.
578 https://doi.org/10.1007/s00338-018-01738-9.

579 Holt, A L., Vahidinia, S., Gagnon, Y.L., Morse, D.E. Sweeney, A.M., 2014. Photosymbiotic giant
580 clams are transformers of solar flux. J. R. Soc. Interface 11, 20140678.
581 https://doi.org/10.1098/rsif.2014.0678.

582 Ip, Y.K., Ching, B., Hiong, K.C., Choo, C.Y.L., Boo, M.V., Wong, W.P., Chew, S.F., 2015. Light
583 induces changes in activities of Na^+/K^+-ATPase, H^+/K^+-ATPase and glutamine synthetase
584 in tissues involved directly or indirectly in light-enhanced calcification in the giant clam,
585 *Tridacna squamosa*. Front Physiol 6, 68. https://doi.org/10.3389/fphys.2015.00068.

586 Ip, Y.K., Hiong, K.C., Goh, E.J.K., Boo, M.V., Choo, C.Y.L., Ching, B., Wong, W.P., Chew, S.F.,
587 2017a. The whitish inner mantle of the giant clam, *Tridacna squamosa*, expresses an apical
588 plasma membrane Ca^{2+}-ATPase (PMCA) which displays light-dependent gene and protein
589 expressions. Front Physiol 8, 781. https://doi.org/10.3389/fphys.2017.00781.

590 Ip, Y.K., Koh, C.Z.Y., Hiong, K.C., Choo, C.Y.L., Boo, M.V., Wong, W.P., Neo, M.L., Chew,
591 S.F., 2017b. Carbonic Anhydrase 2-like in the giant clam, *Tridacna squamosa*:
592 characterization, localization, response to light, and possible role in the transport of
593 inorganic carbon from the host to its symbionts. Physiol. Rep. 5(23), e13494.
594 https://doi.org/10.14814/phy2.13494.

595 Ip, Y.K., Hiong, K.C., Lim, L.J.Y., Choo, C.Y.L., Boo, M.V., Wong, W.P., Neo, M.L., Chew, S.F.,
596 2018. Molecular characterization, light-dependent expression, and cellular localization of
597 a host vacuolar-type H^+-ATPase (VHA) subunit A in the giant clam, *Tridacna squamosa*,
598 indicate the involvement of the host VHA in the uptake of inorganic carbon and its supply
599 to the symbiotic zooxanthellae. Gene 659, 137–148.
600 https://doi.org/10.1016/j.gene.2018.03.054.

601 Ip, Y.K., Hiong, K.C., Teng, J.H.Q. Boo, M.V., Choo, C.Y.L., Wong, W.P., Chew, S.F. 2020a.
602 The fluted giant clam (*Tridacna squamosa*) increases nitrate absorption and upregulates
603 the expression of a homolog of SIALIN (H^+:2NO_3^- cotransporter) in the ctenidium during
604 light exposure. Coral Reefs **39,** 451–465. https://doi.org/10.1007/s00338-020-01907-9.

605 Ip, Y.K., Teng, G.C.Y., Boo, M.V., Poo, J.S.T., Hiong, K.C., Kim, H., Wong, W. P., Chew, S.F.
606 (2020b). Symbiodiniaceae dinoflagellates express urease in three subcellular
607 compartments and upregulate its expression levels in situ in three organs of a giant clam
608 (*Tridacna squamosa*) during illumination. J. Phycol. In press.

609 Jagannathan, L., Cuddapah, S., Costa, M., 2016. Oxidative stress under ambient and physiological
610 oxygen tension in tissue culture. Curr. Pharmacol. Rep. 2, 64–72.
611 https://doi.org/10.1007/s40495-016-0050-5.

612 Jantzen, C., Wild, C., El-Zibdah, M., Roa-Quiaoit. H.A., Haacke, C., Richter, C., 2008.
613 Photosynthetic performance of giant clams, *Tridacna maxima* and *T. squamosa*, Red Sea.
614 Mar. Biol. 155, 211-221.

615 Kliebensten, D.J., Monde, R.N. and Last, R.L., 1998. Superoxide dismutase in *Arabidopsis*: an
616 eclectic enzyme family with disparate regulation and protein localization. Plant Physiol.
617 118, 637–650.

618 Klumpp, D.W., Bayne, B.L., Hawkins, A.J.S., 1992. Nutrition of the giant clam *Tridacna gigas*
619 (L.) I. Contribution of filter feeding and photosynthates to respiration and growth. J. Exp.
620 Mar. Biol. Ecol. 155, 105–122. https://doi.org/10.1016/0022-0981(92)90030-E.

621 Koh, C.Z.Y., Hiong, K.C., Choo, C.Y.L., Boo, M.V., Wong, W.P., Chew, S.F., Neo, M.L., Ip,
622 Y.K., 2018. Molecular characterization of a dual domain carbonic anhydrase from the
623 ctenidium of the giant clam, *Tridacna squamosa*, and its expression levels after light
624 exposure, cellular localization, and possible role in the uptake of exogenous inorganic
625 carbon. Front. Physiol. 9, 281. https://doi.org/10.3389/fphys.2018.00281.

626 Lackner, D.H., Bähler, J., 2008. Translational control of gene expression: from transcripts to
627 transcriptomes. Int. Rev. Cell Mol. Biol. 271, 199–251. https://doi.org/10.1016/S1937-
628 6448(08)01205-7.

629 LaJeunesse, T.C., Parkinson, J.E., Gabrielson, P.W., Jeong, H.J., Reimer, J.D., Voolstra, C.R.,
630 Santos, S.R., 2018. Systematic revision of Symbiodiniaceae highlights the antiquity and
631 diversity of coral endosymbionts. Curr. Biol. 28, 2570–2580.

632 Leggat, W., Badger, M.R., Yellowlees, D., 1999. Evidence for an inorganic carbon concentrating
633 mechanism in the symbiotic dinoflagellate *Symbiodinium* sp. Plant Physiol. 121, 1247–
634 1255.

635 Leggat, W., Buck, B.H., Grice, A., Yellowlees, D., 2003. The impact of bleaching on the metabolic
636 contribution of dinoflagellate symbionts to their giant clam host. Plant Cell. Environ. 26,
637 1951–1961.

638 Lesser, M.P., Stochaj, W.R., Tapley, D.W., Shick, J.M., 1990. Bleaching in coral-reef
639 Anthozoans—effects of irradiance, ultraviolet-radiation, and temperature on the activities
640 of protective enzymes against active oxygen. Coral Reefs 8, 225–32.
641 https://doi.org/10.1007/BF00265015.

642 Lesser. M.P., 1996. Elevated temperatures and ultraviolet radiation cause oxidative stress and
643 inhibit photosynthesis in symbiotic dinoflagellates. Limnol. Oceanogr. 41, 271–283.

644 Muscatine, L., 1990. The role of symbiotic algae in carbon and energy flux in reef corals. Ecosyst
645 World 25, 75–87.

646 Nielsen, D.A., Petrou, K., Gates, R.D., 2018. Coral bleaching from a single cell perspective. ISME
647 J. 12, 1558–1567.

648 Norton, J.H., Shepherd, M.A., Long, H.M., Fitt, W.K., 1992. The zooxanthellae tubular system in
649 the giant clam. Biol. Bull. 183, 503–506.

650 Perl-Treves, R. Galun, E., 1991. The tomato-Cu, Zn-superoxide dismutase genes are
651 developmentally regulated and respond to light and stress. Plant Mol. Biol. 17, 745–760.

652 Perry, J.J.P., Shin, D.S., Getzoff, E.D., Tainer, J.A., 2010. The structural biochemistry of the
653 superoxide dismutases. Biochim. Biophys. Acta, Proteins Proteomics 1804, 245–262.
654 https://doi.org/10.1016/j.bbapap.2009.11.004.

655 Pfannschmidt, T., Allen, J.F., Oelmüller, R., 2001. Principles of redox control in photosynthesis
656 gene expression. Physiol. Plant. 112, 1–9. https://doi.org/10.1034/j.1399-
657 3054.2001.1120101.x.

658 Pochon, X., Wecker, P., Stat, M., Berteaux-Lecellier, V., Lecellier, G., 2019. Towards an indepth
659 characterization of Symbiodiniaceae in tropical giant clams via metabarcoding of pooled
660 multi-gene amplicons. PeerJ 7:e6898. https://doi.org/10.7717/peerj.6898

Poo, J.S.T., Choo, C.Y.L., Hiong, K.C., Boo, M.V., Wong, W.P., Chew, S.F., Ip, Y.K., 2020. Phototrophic potential and form II ribulose-1,5-bisphosphate carboxylase/oxygenase expression in five organs of the fluted giant clam, *Tridacna squamosa*. Coral Reefs 39, 361–374. https://doi.org/10.1007/s00338-020-01898-7.

Rossbach, S., Saderne, V., Anton, A., Durarte, C.M., 2019. Light-dependent calcification in Red Sea giant clam *Tridacna maxima*. Biogeosciences 16, 2635–2650.

Rossbach, S., Subedi, R.C., Ng, T.K., Ooi, B.S., Durarte, C.M., 2020. Iridocytes mediate photonic cooperation between giant clams (Tridacninae) and their photosynthetic symbionts. Front. Mar. Sci. 7:465. https://doi.org/10.3389/fmars.2020.00465

Scandalios, J.G., 1997. Oxidative stress and the molecular biology of antioxidant defences. Cold Spring Harbour Laboratory Press, New York, USA.

Scandalios, J.G., 2005. Oxidative stress: molecular perception and transduction of signals triggering antioxidant gene defenses. Brazilian J. Med. Biol. Res. 38, 995–1014. https://doi.org/10.1590/S0100-879X2005000700003

Sheng, Y., Abreu, I.A., Cabelli, D.E., Maroney, M.J., Miller, A.F., Teixeira, M., Valentine, J.S., 2014. Superoxide dismutases and superoxide reductases. Chem. Rev. 114, 3854–3918.

Sohal, R.S., Dubey, A. 1994. Mitochondrial oxidative damage, hydrogen peroxide release, and aging. Free Radic. Biol. Med. 16, 621–626. https://doi.org/10.1016/0891-5849(94)90062-0

Sturtz, L.A., Diekert, K., Jensen, L.T., Lill, R., Culotta, V.C., 2001. A fraction of yeast Cu, Zn-superoxide dismutase and its metallochaperone, CCS, localize to the intermembrane space of mitochondria: a physiological role for SOD1 in guarding against mitochondrial oxidative damage. J. Biol. Chem. 276, 38084–38089. doi:10.1074/jbc.M105296200

Trench, R.K., 1987. Dinoflagellates in non-parasitic symbiosis. In: Taylor, F.J.Y. (Ed.), The Biology of Dinoflagellates. Blackwell Scientific, Oxford, pp. 530–570.

Tolleter, D., Seneca, F.O., DeNofrio, J.C., Krediet, C.J., Palumbi, S.R., Pringle, J.R., Grossman, A.R., 2013. Coral bleaching independent of photosynthetic activity. Curr. Biol. 23, 1782–1786. https://doi.org/10.1016/j.cub.2013.07.041

Ungvari, Z., Csiszar, A., Sosnowska, D., Philipp, E.E., Campbell, C.M., McQuary, P.R., Chow, T.T., Coelho, M., Didier, E.S., Gelino, S., Holmbeck, M.A., Kim, I., Levy, E., Sonntag, W.E., Whitby, P.W., Austad, S.N., Ridgway, I., 2012. Testing predictions of the oxidative stress hypothesis of aging using a novel invertebrate model of longevity: the giant clam (*Tridacna derasa*). J. Gerontol. A Biol. Sci. Med. Sci. 68, 359–367. https://doi.org/10.1093/gerona/gls159.

Valentine, J.S., Doucette, P.A., Potter, S.Z., 2005. Copper-zinc superoxide dismutase and amyotrophic lateral sclerosis. Ann. Rev. Biochem. 74, 563–593.

Walker, D.W., Benzer, S., 2004. Mitochondrial "swirls" induced by oxygen stress and in the Drosophila mutant *hyperswirl*. Proc. Natl. Acad. Sci. USA 101, 10290–10295. https://doi.org/10.1073/pnas.0403767101.

Xing, Y., Cao, Q., Zhang, Q., Qin, L., Jia, W., Zhang, J., 2013. MKK5 regulates high light-induced gene expression of Cu/Zn superoxide dismutase 1 and 2 in *Arabidopsis*. Plant Cell Physiol. 54, 1217–1227. https://doi.org/10.1093/pcp/pct072.

Compliance with ethical standards

Conflict of interest

On behalf of all authors, the corresponding author states that there is no conflict of interest.

Ethical Approval

All applicable international, national, and/or institutional (Nanyang Technological University) guidelines for the care and use of animals were followed.

Acknowledgements

Funding

This study was funded in part by the Ministry of Education (R-154-000-A37-114 and R-154-000-B69-114) to Y. K. Ip

719 **Table 1.** Percentage similarities between the deduced amino acid sequence of Copper-Zinc
720 Superoxide Dismutase (CuZnSOD) from *Tridacna squamosa* and CuZnSOD sequences from other
721 species obtained from GenBank (accession numbers in parentheses). Sequences are arranged in a
722 descending order of similarity.

Classification	Species	Similarity (%) with CuZnSOD of *T. squamosa*
Molluscs	*Pinctada fucata* CuZnSOD (AFM75822.1)	75.0
	Perna indica CuZnSOD (AGC74195.1)	74.3
	Tegillarca granosa CuZnSOD (ALT54496.1)	74.6
	Mytilus galloprovincialis CuZnSOD (CAQ68509.1)	73.2
	Crassostrea gigas CuZnSOD (CAD42722.1)	73.0
	Mytilus edulis CuZnSOD (CAE46443.1)	72.7
	Ruditapes philippinarum CuZnSOD (AFO64940.1)	67.0
	Sepiella maindroni CuZnSOD (AHJ09887.1)	65.1
	Biomphalaria glabrata CuZnSOD (XP_013070344.1)	62.1
	Octopus vulgaris CuZnSOD (AUR53650.1)	61.7
	Lymnaea stagnalis CuZnSOD (AAP93637.2)	59.6
Teleosts	*Lates calcarifer* CuZnsod (ADT82684.1)	70.3
	Danio rerio CuZnsod (NP_571369.1)	69.6
	Larimichthys crocea CuZnsod (AIL29307.1)	69.6
	Siniperca chuatsi CuZnsod (AHZ96618.1)	69.0
	Oncorhynchus mykiss CuZnsod (NP_001117801.1)	67.0
	Salmo salar CuZnsod (NP_001117059.1)	65.8
Insects	*Musca domestica* CuZnSOD (NP_001295981.1)	68.3
	Drosophila nasuta CuZnSOD (ACL80663.2)	66.4
Mammals	*Bubalus bubalis* CuZnSOD (AHW98673.1)	67.0
	Bos taurus CuZnSOD (NP_777040.1)	67.0
	Sus scrofa CuZnSOD (AHW83665.1)	65.1
	Homo sapiens CuZnSOD (ABL96616.1)	65.1
	Oryctolagus cuniculus CuZnSOD (NP_001076096.1)	64.5
Algae	*Pyropia haitanensis* CuZnSOD (AFX60858.1)	38.1
	Gracilariopsis chorda CuZnSOD (PXF44234.1)	28.7

723

Figure legends

Fig. 1. A multiple amino acid sequence alignment of Copper-zinc Superoxide Dismutase (CuZnSOD) of *Tridacna squamosa* with CuZnSOD sequences from *Perna indica* (Indian brown mussel), *Danio rerio* (zebrafish) and *Homo sapiens* (human). The shaded residues indicate identical or highly similar amino acids. The residues that coordinate the Cu^{2+} are marked with asterisks. The open triangles denote residues which are involved in binding to the Zn^{2+}. The open stars indicate the cysteine residues involved in forming stabilising disulfide bonds. The block arrow points at the gatekeeping residue. CuZnSOD signatures FHVHQYGDN and GNAGGRLACG are indicated by the open boxes.

Fig 2. A phenogramic analysis of Copper-Zinc Superoxide Dismutase (CuZnSOD) of *Tridacna squamosa*, with CuZnSOD sequences from selected mollusks, insects and algae. CuZnSOD of the bacterium, *Pectobacterium atrosepticum*, was used as the outgroup. The number located at each branch point represents the bootstrap value (max=1000).

Fig. 3. The mRNA expression of the host Copper-Zinc Superoxide Dismutase (CuZnSOD) in the outer mantle (OM), inner mantle (IM), ctenidium (CT), foot muscle (FM), byssal muscle (BM), heart (HT), hepatopancreas (HP) and kidney (KD) of *Tridacna squamosa* kept in darkness for 12 h (control). A no template control (NTC) was included in the first lane.

Fig. 4. The transcript level ($\times 10^4$ copies of transcript per ng of total RNA) of the host *Copper-Zinc Superoxide Dismutase (CuZnSOD)* in the (**a**) colorful outer mantle and (**b**) whitish inner mantle of *Tridacna squamosa* kept in darkness for 12 h (control), or exposed to light for 3, 6 or 12 h. Results represent means + S.E.M. (*N*=4).

Fig. 5. The protein abundance of the host Copper-Zinc Superoxide Dismutase (CuZnSOD) in the colorful outer mantle of *Tridacna squamosa* kept in darkness for 12 h (control), or exposed to light for 3, 6 or 12 h. (**a**) Example of an immunoblot of CuZnSOD with tubulin as the reference protein. (**b**) The optical density of the CuZnSOD for a 100 µg protein load was normalized with respect to that of tubulin. Results represent means + S.E.M. (N=4). Means not sharing the same letter are significantly different from each other (P<0.05).

Fig. 6. The protein abundance of the host Copper-Zinc Superoxide Dismutase (CuZnSOD) in the whitish inner mantle of *Tridacna squamosa* kept in darkness for 12 h (control), or exposed to light for 3, 6 or 12 h. (**a**) Example of an immunoblot of CuZnSOD with tubulin as the reference protein. (**b**) The optical density of the CuZnSOD for a 100 µg protein load was normalized with respect to that of tubulin. Results represent means + S.E.M. (N=4).

Fig. 1.

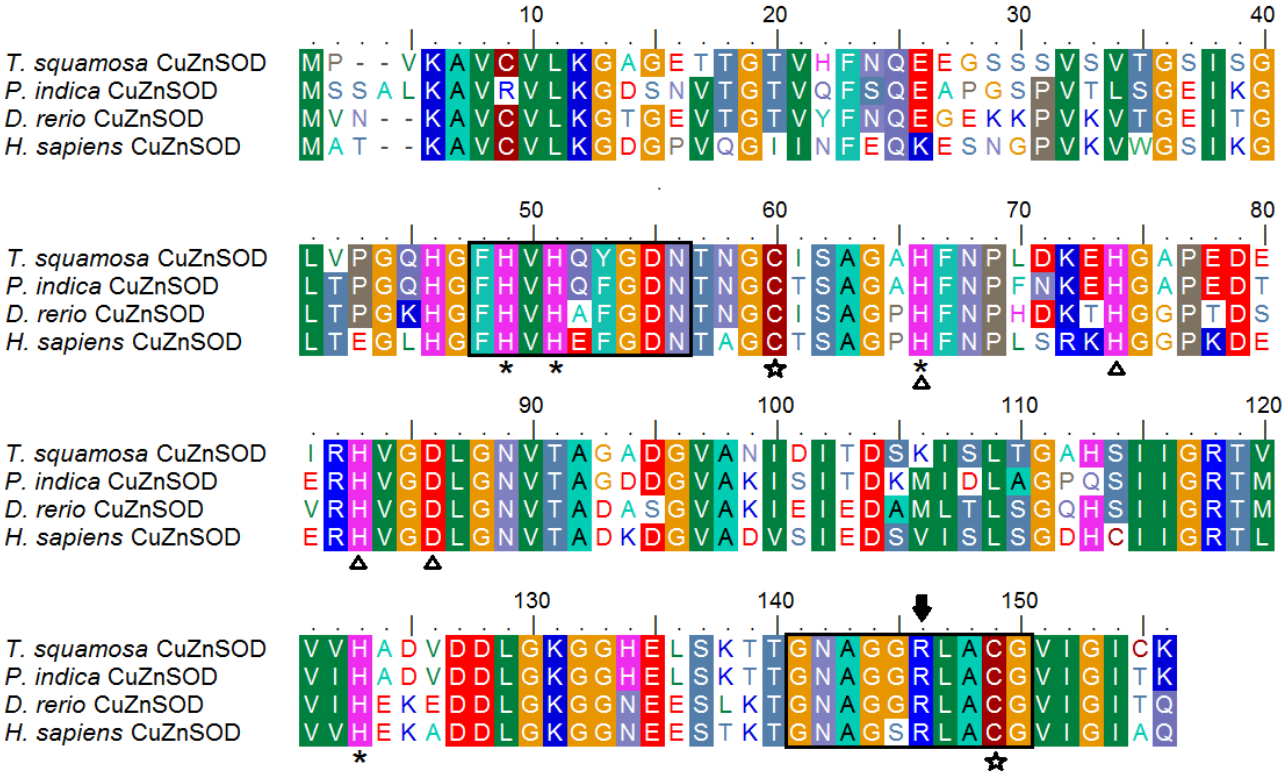
10
20
30
40
T. squamosa CuZnSOD
P. indica CuZnSOD
D. rerio CuZnSOD
H. sapiens CuZnSOD
50
60
70
80
90
100
110
120
130
140
150

34

760

Fig. 2

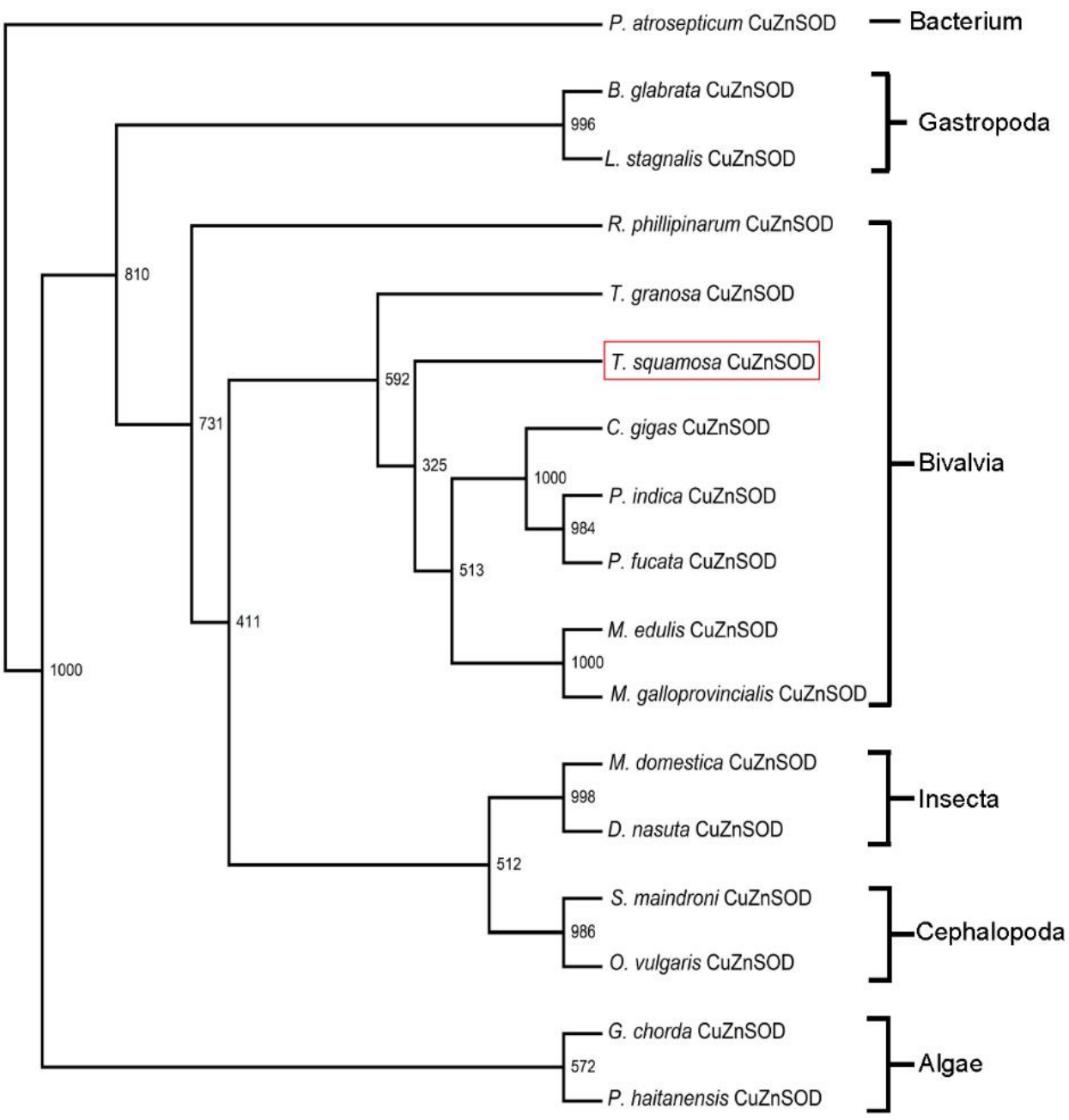
P. atrosepticum CuZnSOD
Bacterium
B. glabrata CuZnSOD
996
L. stagnalis CuZnSOD
Gastropoda
R. phillipinarum CuZnSOD
810
T. granosa CuZnSOD
T. squamosa CuZnSOD
592
731
C. gigas CuZnSOD
325
1000
P. indica CuZnSOD
984
P. fucata CuZnSOD
513
411
M. edulis CuZnSOD
1000
M. galloprovincialis CuZnSOD
Bivalvia
1000
M. domestica CuZnSOD
998
D. nasuta CuZnSOD
Insecta
512
S. maindroni CuZnSOD
986
O. vulgaris CuZnSOD
Cephalopoda
G. chorda CuZnSOD
572
P. haitanensis CuZnSOD
Algae

761

762

Fig. 3.

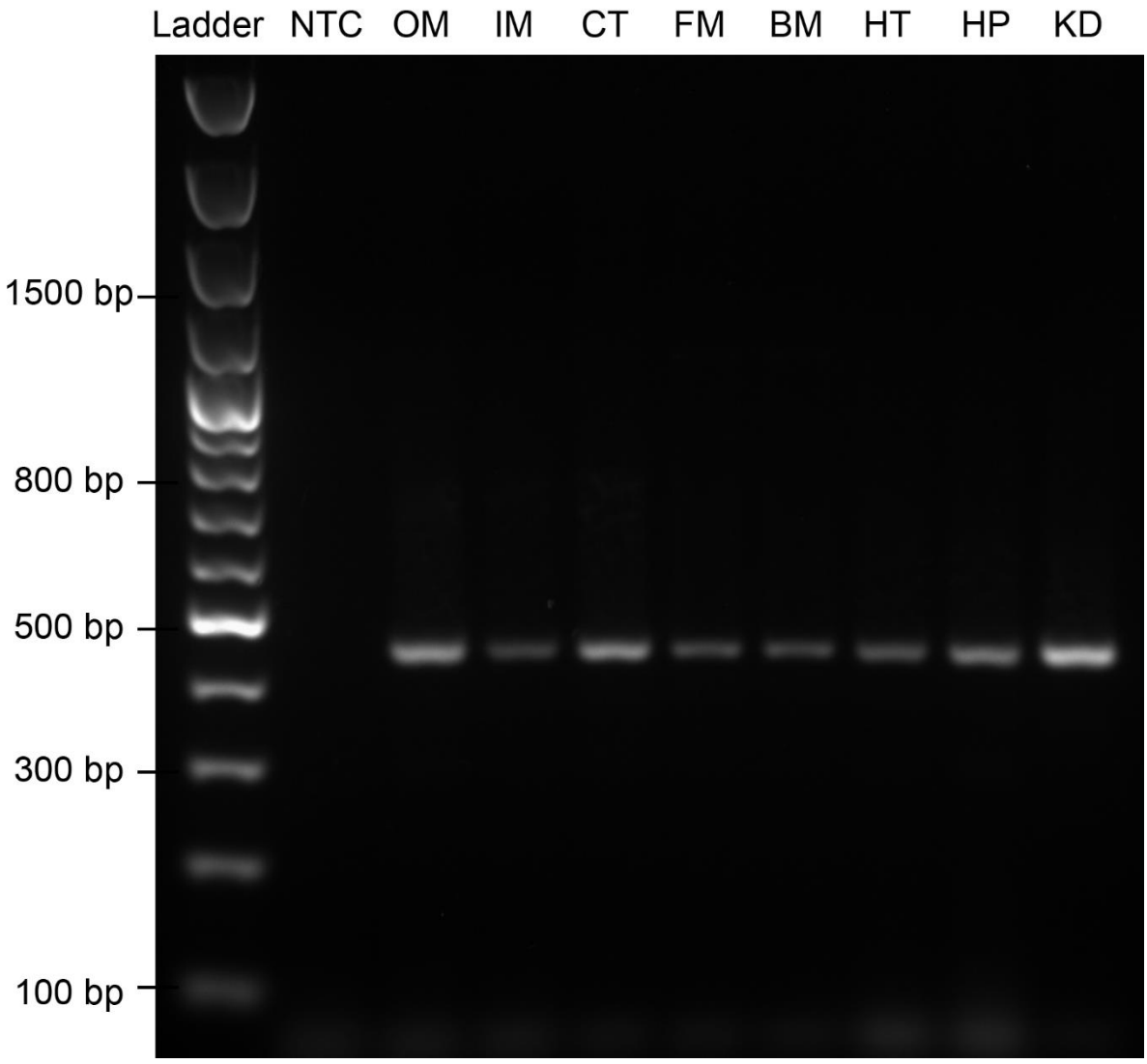

763

764

765 Fig. 4.

766 **a**

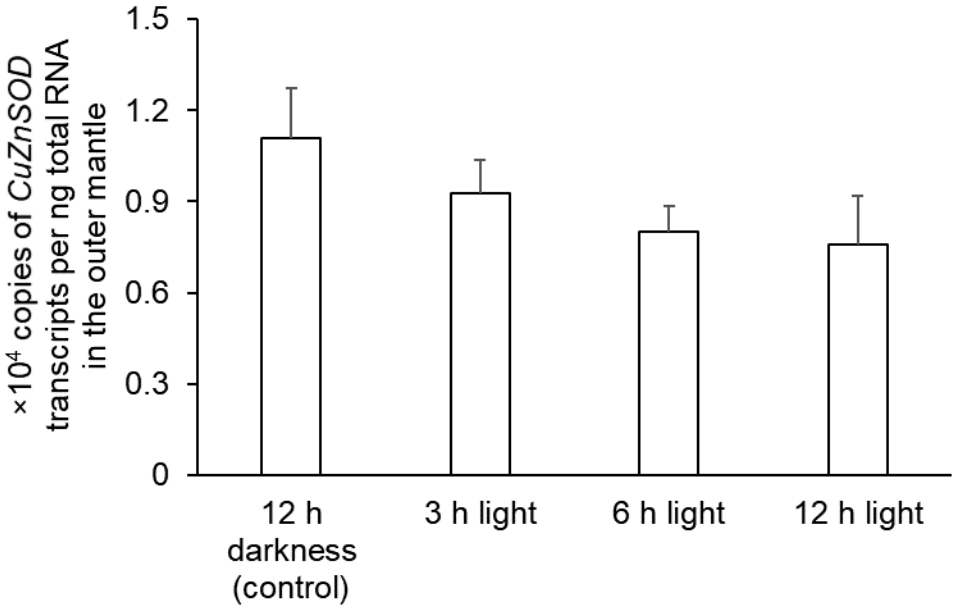

767

768

769 **b**

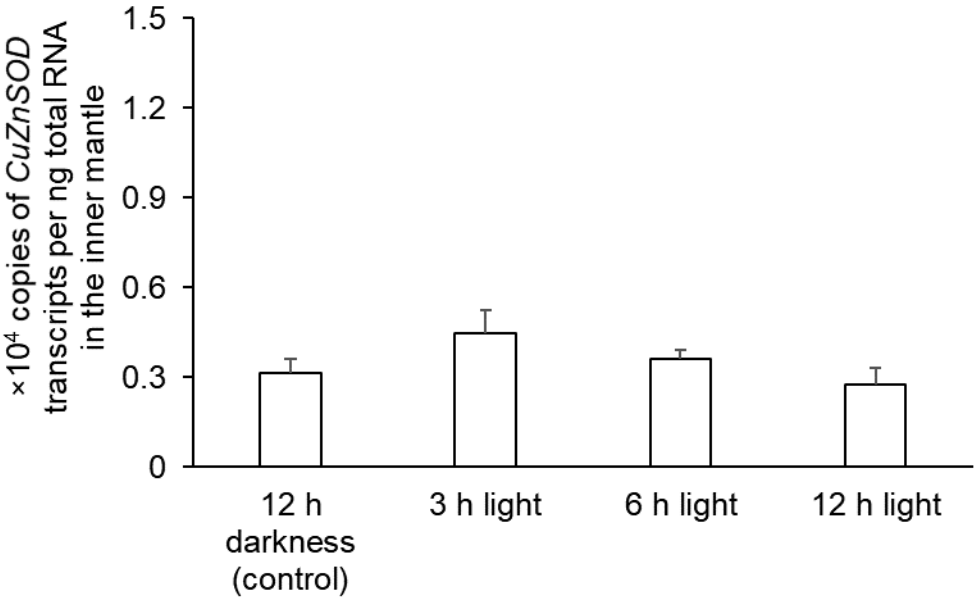

770

771

Fig. 5

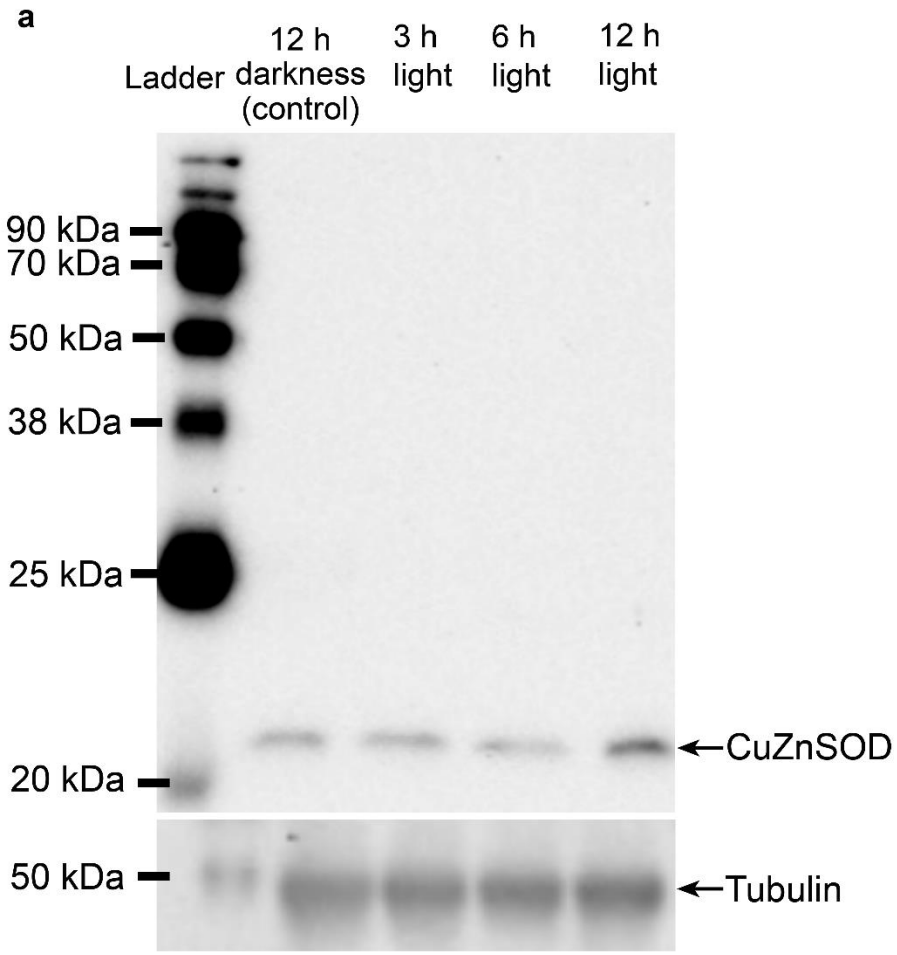
a
Ladder
12 h darkness (control)
3 h light
6 h light
12 h light
90 kDa
70 kDa
50 kDa
38 kDa
25 kDa
20 kDa
CuZnSOD
50 kDa
Tubulin

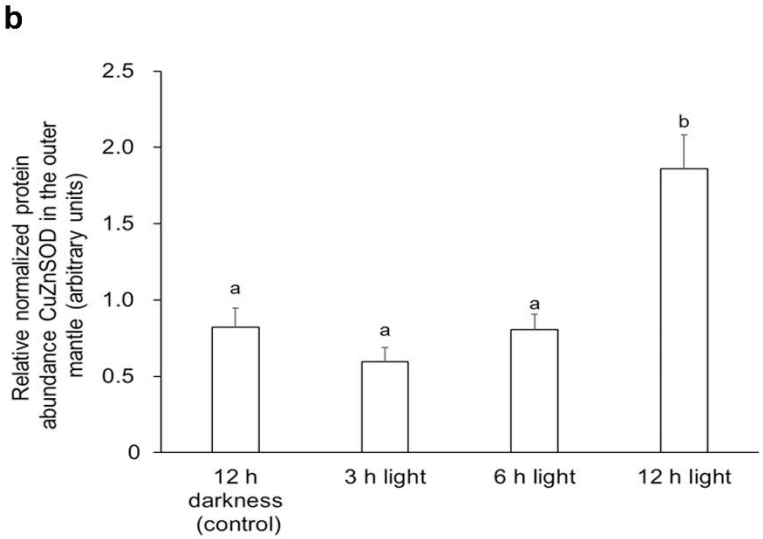
b
Relative normalized protein abundance CuZnSOD in the outer mantle (arbitrary units)
2.5
2.0
1.5
1.0
0.5
0
a
a
a
b
12 h darkness (control)
3 h light
6 h light
12 h light

772

Fig. 6

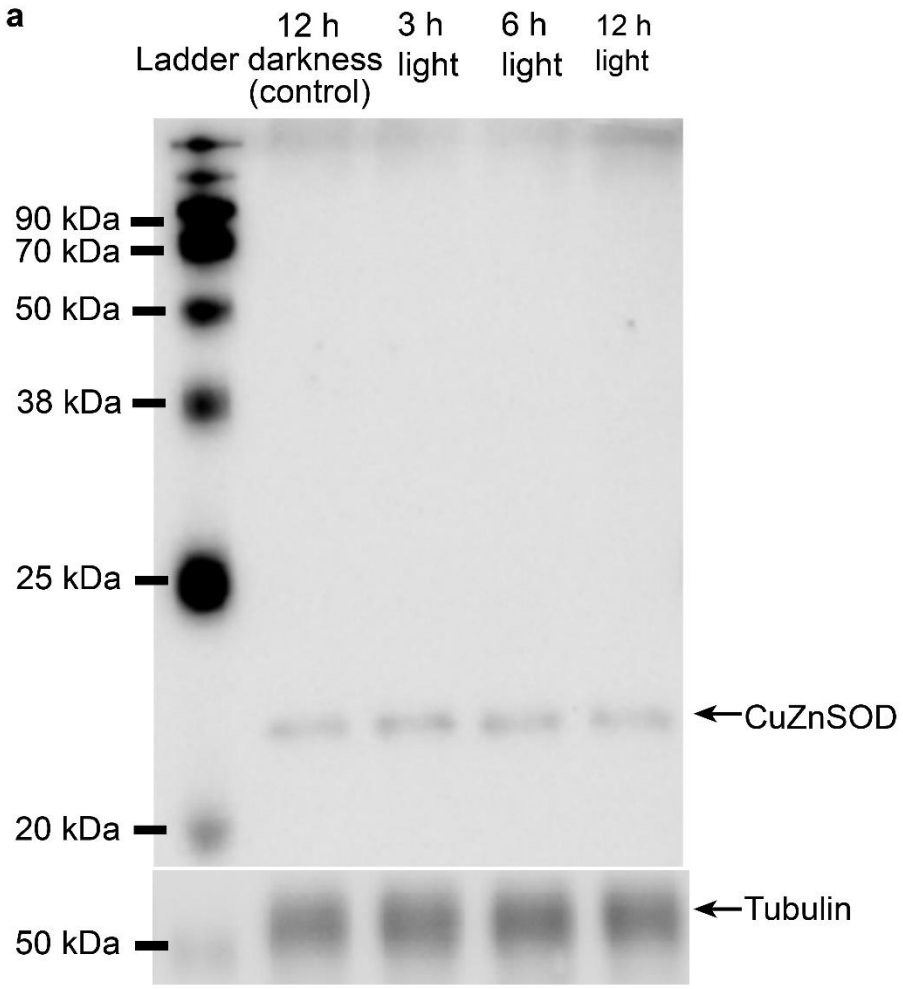
a
Ladder
12 h darkness (control)
3 h light
6 h light
12 h light
90 kDa
70 kDa
50 kDa
38 kDa
25 kDa
20 kDa
50 kDa
CuZnSOD
Tubulin

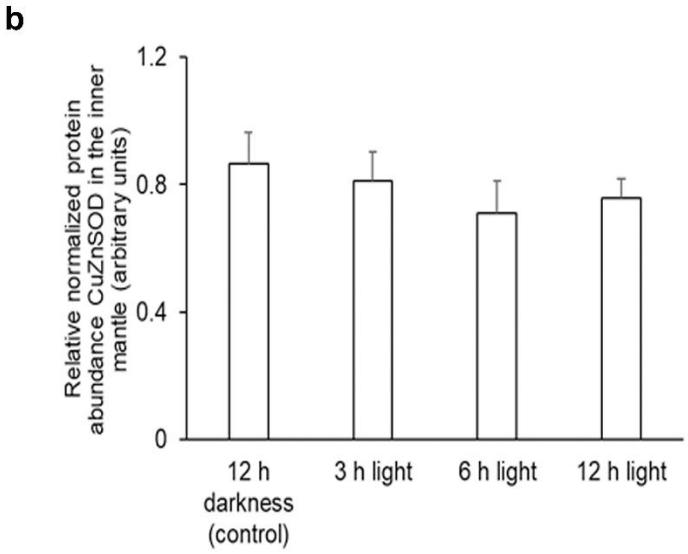
b
Relative normalized protein abundance CuZnSOD in the inner mantle (arbitrary units)
1.2
0.8
0.4
0
12 h darkness (control)
3 h light
6 h light
12 h light

773